Adsorption characteristic of ^{137}Cs from aqueous solution using PAN-based sodium titanosilicate composite

R. Saberi · A. Nilchi · S. Rasouli Garmarodi ·
R. Zarghami

Abstract An organic–inorganic ion exchanger namely sodium titanosilicate-polyacrylonitrile (STS-PAN) composite was synthesized and used for the adsorption of ^{137}Cs from a typical aqueous solution. The physicochemical behavior of the ion exchanger was specified with different techniques including Fourier Transform Infrared Spectroscopy (FT-IR), X-ray powder diffraction (XRD), specific surface analysis (BET), thermogravimetry-differential scanning calorimetry (TG-DSC), scanning election microscopy (SEM), X-Ray Fluorescence spectroscopy (XRF) and CHN elemental analysis. The thermal and gamma irradiation stability of the synthesized ion exchanger was investigated. It was observed that the ion exchanger is stable up to 275 °C and against gamma irradiation up to 200 KGy. The effects of pH, contact time, ambient temperature, and presence of various cations on adsorption rate of STS-PAN were also studied and the optimum conditions obtained. In addition, thermodynamic parameters were evaluated during the adsorption. The values of the enthalpy and the Gibbs free energy suggest an endothermic and spontaneous process. Adsorption isotherm in batch experiment showed that the sorption data were successfully fitted with Langmuir model. Finally the adsorption dynamic capacity of the synthesized composite in a columnar experiment as well as its elution was evaluated. The complete breakthrough curve was generated at a feed rate of 15 bed volume per hour and sorbent capacities were obtained at 5 and 100% breakthrough.

Keywords ^{137}Cs · Ion exchanger · Adsorption · Sodium titanosilicate · Polyacrylonitrile

R. Saberi
Department of Environment and Energy, Science and Research Branch, Islamic Azad University, Tehran, Iran

A. Nilchi (✉) · S. Rasouli Garmarodi
Nuclear Science and Technology Research Institute, P.O. Box 11365-8486, Tehran, Iran
e-mail: anilchi@aeoi.org.ir

R. Zarghami
School of Chemical Engineering, College of Engineeing, University of Tehran, P.O. Box 11155-4563, Tehran, Iran

Introduction

There are a number of liquid processes and waste streams at nuclear facilities that require treatment and/or the removal of radioactive contaminants. Cesium and strontium are the most abundant radionuclides in nuclear fission products that are routinely or accidentally released. They have relatively long half-life of about 30 years and are considered as hazardous elements for the environment. Ion exchange technique has become one of the most commonly used treatment methods for such aqueous streams due to its simplicity, selectivity and efficiency. A wide range of materials having different chemical and physical properties, which can be naturally occurring or synthetic, is available for this technique [1–11].

Several inorganic ion exchangers such as zeolites, sodium titanates, silicotitanates, metal oxides and hexacyanoferrates are in use in nuclear sites for the treatment of nuclear wastes. However, the slow mass-transfer rate in column operation has been the impeding factor for extensive applications. On the other hand, the application of organic ion exchange resins to the wastes treatment has been decreased because they possibly release the radionuclides by decomposition of organic binding matrix when disposed underground. These reasons have recently expedited the

study on the preparation and the application of organic–inorganic composite ion exchangers for the treatment of various radioactive and industrial waste waters. In composite ion exchanger, inorganic materials are active components to which all the radionuclides are bound and organic materials are simply inert binders. Therefore, contrary to the organic ion exchange resins, even in the case of decomposition of organic binding matrix, no radionuclides are released [12, 13].

Polyacrylonitrile (PAN) is reportedly one of the most favorable organic binders, due to its characteristic features such as excellent pelletizing property, good solubility for organic solvents, strong adhesive forces with inorganic materials and chemical stability [14]. PAN beads are highly porous and can accommodate very high loadings of ion exchange material (5–95%) into the PAN matrix. These highly porous PAN beads exhibit a number of advantages over other granular sorbents. These advantages include significantly improved kinetics and sorbent capacity owing to the increased availability of the sorbent material, easy modification of physico-chemical properties (hydrophilicity, porosity, mechanical strength) and simplified production. Several authors published papers on the use of PAN as a binding polymer for granulating different inorganic cation exchangers [15–18]. Todd et al. used PAN-AMP containing ammonium molybdophosphate granulated with PAN to study the uptake of cesium from concentrated acidic wastes [19]. Also Zn and Cu hexacyanocobaltates was supported on PAN and used successfully for removal of the radioactive cesium from different aqueous solutions [20].

This paper presents the preparative conditions, adsorption properties and analytical applications of sodium titanosilicate-polyacrylonitrile polymeric-inorganic composite material used as a cation exchanger for removal of ^{137}Cs from aqueous solutions.

Experimental

Reagents and apparatus

All the reagents and chemical used were of analytical grade obtained from Merck, Fluka, and Aldrich. Radioactive tracer ^{137}Cs was supplied by Nuclear Science and technology Research Institute of Iran and subsequently used to label the Cs$^+$ solutions of desired concentrations prepared by dilution of 0.1 mol/L Cs$^+$ stock solution.

The infrared spectra was recorded using a Brucker-Vector 22 spectrophotometer; X-ray powder diffractometry was carried out using an 1800 PW Philips diffractometer with CuKα beam in order to determine the structure of the adsorbers. The X-ray source was a rotating anode operating

at 40 kV and 30 mA with a copper target and the data were collected between 5 and 70° in 2θ; Brunauer–Emmett–Teller (BET) specific surface area was determined through nitrogen adsorption isotherms using Quantachrome NOVA 2200e system; Scanning electron microscope (SEM) imaging was performed by means of a Philips XL30; thermogravimetry-differential scanning calorimetry (TG-DSC) were carried out on heating the sample up to 800 °C at a heating rate of 10 °C/min in the Argon atmosphere using a DuPont model 951; carbon, hydrogen and nitrogen contents of the composite was determined using an Elementar-Vario ELIII, CHN elemental analyzer; the amount of Na$^+$, K$^+$, Ca^{2+} and Mg^{2+} cations was measured by a Perkin Elmer atomic absorption spectrometer (AAS) model 843; The X-Ray Fluorescence Unit (Oxford ED 2000) which is used to determine the amount of titanium and silicon, the radioactivity was counted using a high purity germanium detector gamma spectrometer Ortec model GMX-15185-5 and finally the pH measurement were made with a Schott pH-meter model CG841.

Preparation of composite adsorbent

For sodium titanosilicate preparation, 39 mL of 6 mol/L NaOH solution was added to 6.8 g of tetraethyl orthotitanate 97% and 5.0 g of tetraethyl orthosilicate 99%. The synthesis was carried out under hydrothermal conditions at temperature 150 °C for 5 days. The precipitate was filtered and washed with distilled water then ethanol. The solid was then dried at 100 °C and sieved to size of 224–400 μm.

For composite beads preparation; the weighed amount of sodium titanosilicate powder was mixed with the solvent dimethylsulfoxide (DMSO) and a few drops of Tween-80 surfactant and stirred at 50 °C for 3 h. Then, 2.4 g of polyacrylonitrile powder were added to this solution with stirring at 50 °C for 4 h to obtain homogeneous solution of the composite dope. The dissolved air in the dope was removed by vacuum pump, and the air-free composite dope as described in previous study, was passed through inside the dual nozzle while the compressed air was ejected through the outside annulus of the dual nozzle to adjust the size of the composite beads [21]. The ejected composite beads were then dropped in distilled water, which was used as a gelation agent. Finally, the beads were washed using demineralized water and dried at 50 °C. The bead sizes were varied in the range of 2–3 mm with the air pressure variation.

Experimental procedure

The adsorption experiments have been studied by batch technique. 0.1 g of the prepared composite ion exchanger and 10 mL of the labeled 10^{-4} mol/L cesium solution of

desired pH were shaken with uniform speed using a thermostated shaker bath. pH of the adsorptive solutions was adjusted with the suitable quantity of NaOH and HCl, monitored with a digital pH meter. All experiments were carried out at 25 °C except for the temperature dependence studies where temperature varied from 25–65 °C. Before adding the adsorbent, an aliquot of the bulk solution was withdrawn for the measurement of the initial radioactivity. For the evaluations of distribution coefficient (K_d) of cesium as a function of contact time, from 5 to 120 min time intervals were applied. At the end of each time interval, the solution was filtered for phase separation and the radioactivity of supernatant solutions was measured, then K_d for adsorbed cesium on the composite was determined from the following equation:

$$K_d = \frac{R_o - R_e}{R_e} \times \frac{V}{m} (mL/g) \qquad (1)$$

where R_o and R_e are radioactivity in the initial and equilibrium stages, V the solution volume (mL) and m is the mass of sorbent (g).

Also the same experimental conditions were applied in order to investigate the influence of Na$^+$, K$^+$, Ca^{2+} and Mg^{2+} cations on the distribution coefficient (K_d) of cesium.

The sorption isotherm experiments were conducted at the temperature of 25 °C and pH 6.0 (±0.1) by batch sorption procedure. 0.1 g of adsorbent was mixed with 10 mL samples of different initial concentration of Cs$^+$ solution and were shaken in order an equilibrium could be achieved.

Results and discussion

Synthesized composit characteristics

Figure 1 depicts XRD patterns of three synthesized materials: (a) Polyacrylonitrile, (b) STS, and (c) STS-PAN. The analysis of X-ray patterns revealed that the XRD data corresponding to the synthetic STS agreed well with previously reported papers [22, 23]. It was also observed that no diffraction peaks can be seen in the pattern of polyacrylonitrile which indicates an amorphous structure but the 2θ values at the peak points of STS-PAN are the same as those in STS, and hence their crystalline structure is very similar. Using the above facts, it was determined that STS-PAN composition has been accurately synthesized.

The IR spectrum of STS-PAN composite is recorded in Fig. 2. The broad band in the region of 2800–3650 cm^{-1} is due to interstitial water and hydroxyl groups and the sharp peak at 1650 cm^{-1} corresponds to the bending vibration of water molecules. Absorption peak at 495 cm^{-1} can be assigned to the bending vibration of Ti–O. The spectrum of the sample shows the characteristic band for –CH$_2$ at
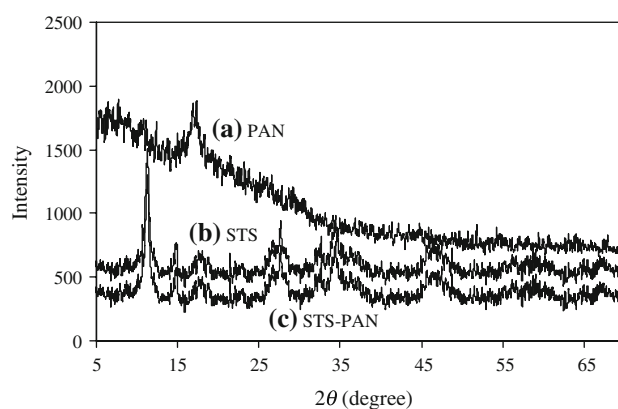
Fig. 1 XRD patterns of synthesized materials: (*a*) Polyacrylonitrile, (*b*) STS, and (*c*) STS-PAN composite
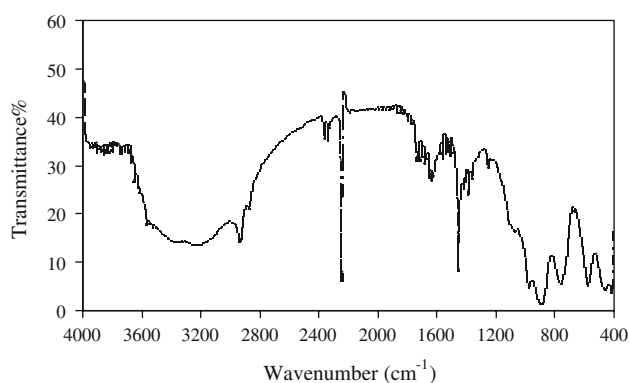
Fig. 2 IR spectrum of STS-PAN composite

1465 cm^{-1}. The band at 950 cm^{-1} is assigned to the Si–O–Ti bond stretching vibration in exchanger structure. The bands in the 750 cm^{-1} region are due to the Si–O vibration in the synthesized composite. Finally, the sharp peak in 2250 cm^{-1} can be assigned to the nitrile group.

The nitrogen adsorption–desorption studies showed that the BET surface area of sodium titanosilicate—polyacrylonitrile composite is 96.66 m^2/g.

Scanning electron microscope (SEM) imaging of the prepared STS-PAN composite bead is shown in Fig. 3. To take SEM photographs, electrons are usually accelerated within a range of 1–30 keV. This image indicates that the pore size of the inner part of the particles was larger than that near the surface. The kinetic of sorption on these adsorber beads must be very fast, since the STS powder which is the active material for adsorption, is found to be dispersed throughout the binding matrix. In other word, this image indicates the structure of synthesized STS is tunnel-shaped with a high adsorption level.

Using a CHN unit, elements of carbon, hydrogen and nitrogen contained in the composite were measured, and XRF spectroscopy was used to determine the amount of titanium and silicon. The results achieved are shown in Table 1.
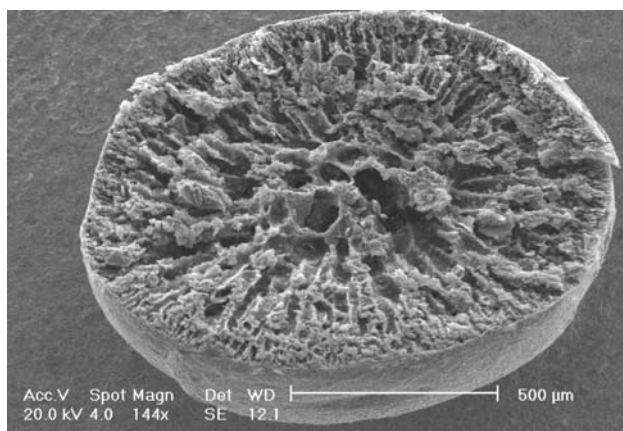
Fig. 3 Three dimensional scanning electron microscopic photograph of STS-PAN composite cross-section

Table 1 Analytical results of the synthesized composite elements

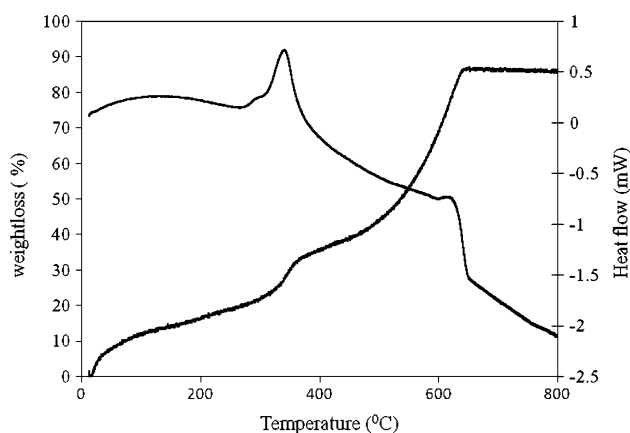| Element	Weight (%)
Ti	34.50
Si	13.60
C	32.78
H	3.78
N	6.54

Fig. 4 TGA-DSC curves of synthesized composite

The TGA-DSC thermal analysis of STS-PAN composite is shown in Fig. 4 which shows decomposition steps. This Figure demonstrates that weight reduction up to 275 °C occurs due to elimination of free water molecules; and above this temperature (275–370 °C); structural collapse of polymers contained in the composite will cause reduction of adsorbent weight. Finally, in temperatures between 370–655 °C, weight reduction is due to release of space lattice water molecules outward and emission of hydrogen cyanide (HCN) gas from the synthesized compound. Therefore, sodium titanosilicate-polyacrylonitrile is stable up to 275 °C.

Stability of STS-PAN against gamma irradiation

Through assessment of IR spectrum of STS-PAN composite, probable variations in the exchanger structure as a result of gamma rays can be predicted. IR spectra of the sample prior to gamma irradiation (100 and 200 KGy doses) and after that were compared.

As it can be seen in Fig. 5, no change is observed among IR spectra of all three samples (a-unpredicted by gamma, b- gamma-irradiated up to 100 KGy, c-gamma-irradiated up to 200 KGy); in the other words, the synthesized composite will be stable against gamma irradiation up to 200 KGy under which no change occurs through the composite's structure.

Adsorption characteristics

Effect of contact time

Pursuant to the assessment of factors having impact on cesium adsorption, the influence of contact time between cesium solution and STS-PAN on distribution coefficient of cesium was investigated. As it can be seen in Fig. 6, the adsorption rate soars with time increase, and equilibrium is maintained between two phases after about 130 min. In the subsequent experiments, the contact time of 130 min was selected for sorption equilibration of Cs^+ on STS-PAN.

Effect of solution initial pH

The effect of pH on the sorption of Cs^+ ions from aqueous solutions using the prepared composite material was investigated over the pH range of 1.0–9.0 (Fig. 7). It was observed that the distribution coefficient of cesium continuously increases with increasing pH and the optimum pH value at which the maximum adsorption could be achieved was 6.0. Low distribution coefficient in acidic environments can be attributed to competition of H^+ cations with cesium ions for the exchange sites in the adsorbent.
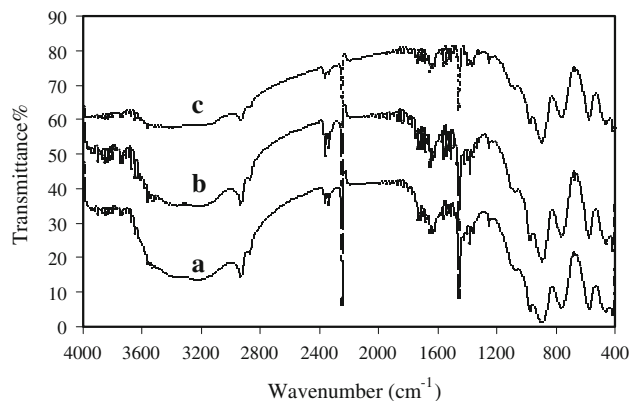

Fig. 5 IR spectra comparison over modes of (*a*) unpredicted (*b*) irradiated up to 100 KGy and (*c*) irradiated up to 200 KGy
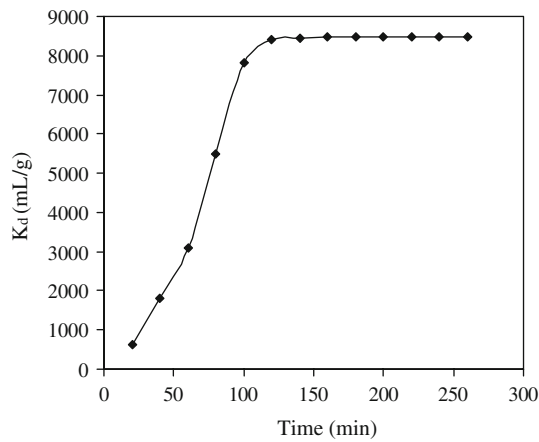
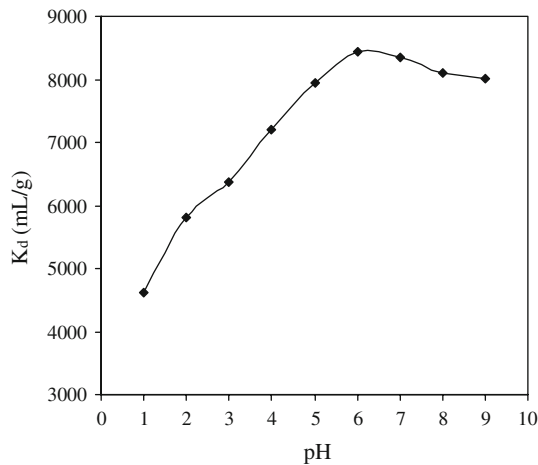**Fig. 6** Variation of distribution coefficient of cesium with contact time

Fig. 7 Variation of distribution coefficient of cesium with PH of the solution

Table 2 The effect of the added cations in the solution on the distribution coefficient of cesium ions on STS-PAN

Added cation	K_d (mL/g)
Nil	8406
Na$^+$	1836
K$^+$	1287
Ca^{2+}	2406
Mg^{2+}	2721

Effect of other cations

Change of distribution coefficient values of Cs$^+$ cation along with the tracer was evaluated in the presence of Na$^+$, K$^+$, Ca^{2+} and Mg^{2+} cations at 10^{-4} mol/L concentration added in the form of their nitrates at 298 K. The results (Table 2) indicate that the distribution coefficient of cesium has decreased in the presence of added cations.

Effect of solution temperature

The effect of medium temperature of distribution coefficient with regard to Cs$^+$ cation was examined, while other parameters were kept constant (adsorptive concentration for Cs$^+$ 10^{-4} mol/L and pH 6.0).

The results obtained in Table 3 reveal that rising of the medium temperature from 298 K to 338 K (from 25 °C to 65 °C), in steps of 10 K (10 °C), brings about positive impact on the magnitude of distribution coefficient. As temperature goes up, the required energy for precipitation of hydrated cations layers is provided, and it also leads to enhancement of cations motion existing in exchanging network and facilitates the interaction. Therefore, the above exchanging process is endothermic.

Process thermodynamic parameters

Variation of standard thermodynamic parameters during the adsorption process was evaluated using the following equations [24]:

$$\ln K_d = \frac{-\Delta H^\circ}{RT} + \frac{\Delta S^\circ}{R} \tag{2}$$

where ΔH°, ΔS° and T are the standard enthalpy, standard entropy, and temperature in Kelvin, respectively, and R is the gas constant. Considering the above equation and by drawing Ln K_d diagram in terms of $1/T$, values of ΔH° and ΔS° are determined. The values of enthalpy and entropy can be obtained from the slope and intercept of linear variation of ln K_d with reciprocal temperature (Fig. 8). The standard Gibbs free energy, ΔG°, of specific adsorption was calculated from the well-known equation:

$$\Delta G^\circ = \Delta H^\circ - T\Delta S^\circ \tag{3}$$

The values of $\Delta \mathring{H}$ and ΔG° are presented in Table 4. Table 4 reveals that the value of $\Delta \mathring{H}$ is positive and the value of ΔG° is negative which show that the sorption of cesium on synthesized composite is an endothermic and a spontaneous ion-exchanging process.

Adsorption isotherms

The adsorption isotherm is the equilibrium relationship between the concentration in the fluid phase and the

Table 3 The effect of solution temperature on the distribution coefficient of cesium ions on STS-PAN

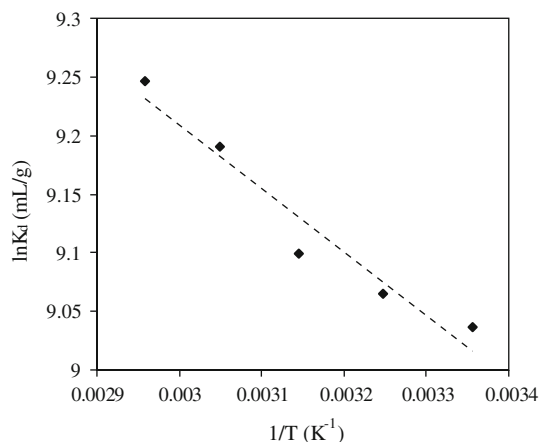| Temperature (K)	K_d (mL/g)
298	8406
308	8649
318	8952
328	9801
338	10362

Fig. 8 The effect of solution temperature on the distribution coefficient of cesium ions on STS-PAN

Table 4 Thermodynamic parameters for cesium adsorption on the synthesized STS-PAN

$\Delta \overset{\circ}{H}$ (kJ/mol)	4.5177
$\Delta \overset{\circ}{S}$ (kJ/K mol)	0.0809
$\Delta \overset{\circ}{G}$ (kJ/mol)	
298 K	19.6165
308 K	20.4264
318 K	21.2363
328 K	22.0462
338 K	22.8560

concentration in the adsorbent particles at a given temperature and pH. The adsorption isotherm parameters show actually the surface properties and affinity of the sorbent. Some typical isotherm shapes are shown in the literature as arithmetic graphs. In this paper Langmuir and Freundlich models are applied to calculate the sorption data of Cs^+ on STS-PAN.

The Langmuir sorption isotherm has been widely used to characterize the adsorption phenomena from solution. The isotherm is valid for monolayer adsorption onto a surface containing a finite number of identical sites. The form of Langmuir isotherm can be represented by the following equation [25]:

$$\frac{C_e}{q_e} = \frac{1}{Q^\circ b} + \frac{C_e}{Q^\circ} \tag{4}$$

where q_e is the amount of metal ion sorbed per unit weight of adsorbent (mol/g), C_e the equilibrium concentration of the metal ion in the equilibrium solution (mol/L), Q° the monolayer adsorption capacity and b is the constant that relates to the heat of adsorption.

Freundlich isotherm model stipulate that the ratio of solute adsorbed to the solute concentration is a function of the solution. This model allows for several kinds of sorption sites on the solid and represents properly the sorption
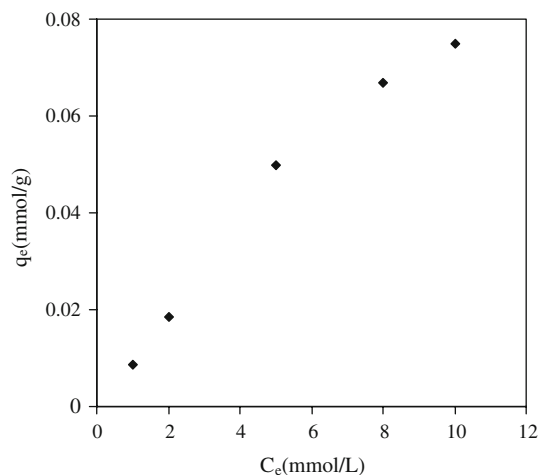
data at low and intermediate concentrations on heterogeneous surfaces. The model has the following form [26]:

$$\log q_e = \log K_F + \frac{1}{n} \log C_e \tag{5}$$

where K_F represents the sorption capacity when metal ion equilibrium concentration equals to 1, and $1/n$ represents the degree of dependence of sorption with equilibrium concentration.

Figure 9 represents the experimental adsorption isotherm of the intended composite and Figs. 10 and 11 demonstrate the fitted resulting diagrams based on Langmuir and Freundlich equations at 25 °C (298 K). The parameters calculated from the slopes and the intercepts, by means of a linear least square fitting method, are summarized in Table 5. Higher correlation coefficient indicates that the cesium adsorption on the synthesized STS-PAN composite is monolayer and the Langmuir model fits the
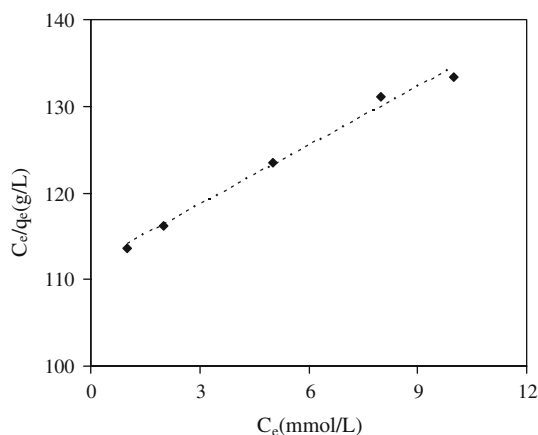

Fig. 9 Adsorption isotherm of cesium on STS-PAN composite at 298 K

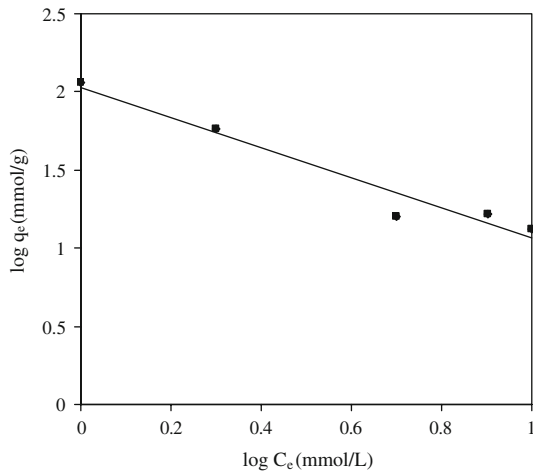Fig. 10 Langmuir adsorption isotherm of cesium on STS-PAN composite at 298 K

Fig. 11 Freundlich adsorption isotherm of cesium on STS-PAN composite at 298 K

Table 5 The parameters of Langmuir and Freundlich isotherms STS-PAN composite at 298 K

Langmuir constants	$Q°$ (mmol/g)	0.440
	b (L/mmol)	0.020
	R^2	0.990
Freundlich constants	K_F (mmol/g)(L/mmol)$^{1/n}$	0.009
	$1/n$	0.960
	R^2	0.953

adsorption data better than the Freundlich model over the entire range of adsorptive concentration studied.

Columnar experiments

Breakthrough diagram

In column fixed bed adsorption, the concentrations in the fluid phase and the solid phase change with time as well as with position in the bed. At first time, most of the mass transfer takes place near the inlet of the bed, where the fluid contact fresh adsorbent. If the solid contains no adsorbate at the start, the concentration in fluid drops exponentially with distance essentially to zero before the end of the bed is reached. After a few minutes, the solid near the inlet is nearly saturated, and most of mass transfer takes place further from the inlet.

In this stage also 0.2 g of STS-PAN composite was put in glass tubes with 0.8 cm diameter and 60 cm long. Then 200 mL of effluent containing Cs^+ together with tracer, with 50 ppm concentration was passed through the tube. The concentration gradient, A_i/A_f, becomes S-shaped versus time, where A_i is Cs effluent activity (Bq/mL) and A_f is Cs feed activity (Bq/mL). Cesium breakthrough curve was generated from columnar test A_i/A_f, by plotting the number

Table 6 Water characteristics of sample water

TDS (mg/L)	E °C (μS/Cm)	pH	K^+ (mg/L)	Na^+ (mg/L)	Mg^{2+} (mg/L)	Ca^{2+} (mg/L)
200	34	8.36	1.17	10.35	10.56	50.2

of bed volumes (BV) of feed processed against the percent breakthrough $A_i/A_f \times 100\%$. The region where most of the change in concentration occurs is called the mass transfer zone, and the limits are often taken as A_i/A_f, equal to 0.95 to 0.05.

Solutions were made using water sample taken from river near capital city of Iran, Tehran. Table 6 represents the analytical results of its water. It is noteworthy that this river is seasonal, so during the other seasons has little water or is even dry.

Figure 12 shows breakthrough curve on STS-PAN composite. To provide an estimate of dynamic capacity, a second order kinetic equation was fit to the data set to obtain a relationship for Cs effluent concentration as function of throughput volume. This equation for Cs concentration was then substituted into following relationship for dynamic capacity (DC):

$$DC = \frac{\int_0^v (A_f - A_i) dv}{M} \tag{6}$$

where v is volume at specified breakthrough, and M is mass of STS-PAN sorbent (g dry). Dynamic capacity estimated was then obtained by evaluating the integral numerically with upper limit values corresponding to approximately 5 and 100% Cs breakthrough. Adsorption dynamic capacity of the synthesized composite in 5 and 100% breakthrough conditions, as well as efficiency of the adsorbent column are presented in the following Table 7. Though the structure of synthesized adsorbent is tunnel-shaped with a very high adsorption level, it is observed that cesium adsorption rate is
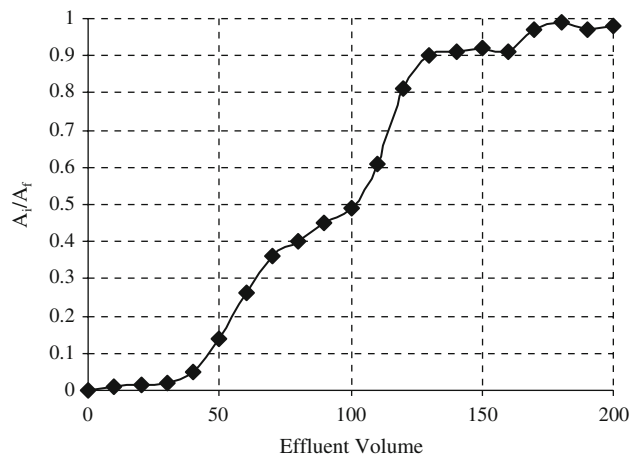

Fig. 12 Breakthrough diagram of cesium on STS-PAN composite for a sample river water

Table 7 Adsorption dynamic capacity in columnar experiment on STS-PAN adsorbent using river water sample

Flowrate (bed volume/h)	Dynamic capacity at 5% breakthrough (practical)	Dynamic capacity at 100% breakthrough (total)	Efficiency of adsorbent column (%)
15	9.80 mg Cs/g STS-PAN	22.06 mg Cs/g STS-PAN	44.42
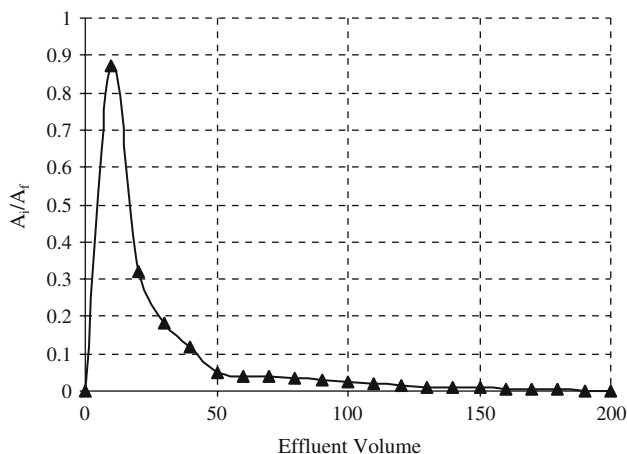
Fig. 13 Elution curve of cesium from STS-PAN composite with 0.1 normal HCL solution

not so high on the synthesized adsorbent, which this phenomenon is due to high reluctance of sodium ion contained in the adsorbent structure to interact with cesium ion contained in the solution. Due to high contamination of ^{137}Cs ion, practically higher than 5% saturation is used. Sorbent capacities at a flow rate of 15 BV/hr were determined to 9.80 and 22.06 mg Cs/g STS-PAN 5 and 100% Cs breakthrough, respectively. The efficiency formula of adsorbent column is:

$$E = \frac{\text{Area 1}}{\text{Area 1} + \text{Area 2}} \times 100 \qquad (7)$$

where area 1 is the area above the curve from $A_f/A_i = 0\%$ till $A_f/A_i = 5\%$, and area 2 is the area above the curve from $A_f/A_i = 5\%$ to $A_f/A_i = 100\%$, the obtained efficiency is approximately about 44.42%.

Elution diagram

For elution studies, a glass column containing 0.2 g of the prepared composite on a glass wool support was loaded with a solution of 10^{-4} mol/L containing ^{137}Cs tracer. Desorption with 0.1 mol/L HCl solution was carried out at a flow rate of 0.5 mL/min at 25 °C. Fractions of 10 mL were analyzed for ^{137}Cs activity. Figures 13 shows elution curve of cesium from STS-PAN composite with 0.1 normal HCL solution. As it can be seen about 85% of the adsorbed Cs was eluted with 50 mL eluent. This confirms the

difficulties are not encountered in eluting cesium from STS-PAN composite.

Conclusions

The studies showed that the synthesized composite have crystalline structure and was thermally stable, resistant to gamma irradiation of up to 200 KGy. The adsorption properties showed that the adsorption of cesium is directly depended upon the contact time, temperature and pH of the media used, and as these controlling parameters increase, the adsorption of cesium ions for the ion exchanger, increase. The equilibrium data obtained in this study accorded excellently with the Langmuir adsorption isotherm over the entire concentration range investigated. The values of $\Delta \mathring{G}$, $\Delta \mathring{H}$ and $\Delta \mathring{S}$ prove that the sorption of cesium on STS-PAN is an endothermic and a spontaneous process. The overall results indicate the possibility of using the synthesized composite for efficient removal of ^{137}Cs from aqueous solutions. Furthermore, its spherical shape allows it to be used successfully in column separation processes. Complete breakthrough curve was generated at feed rate of 15 BV/hr and sorbent capacities were determined to be approximately 9.80 and 22.06 mg Cs/g STS-PAN, 5 and 100% Cs breakthrough, respectively. In this case the column efficiency was 44.42%. Finally, the elution result confirms that the STS-PAN has good elution characteristic.

References

1. Zhang A, Xiao C, Xue W, Chai Z (2009) Chromatographic separation of cesium by a macroporous silica-based supermolecular recognition agent impregnated material. Sep Purif Technol 66:541–548
2. Oancea AMS, Popescu AR, Radulescu M, Weber V, Pincovschi E, Cox M (2008) Kinetics of cesium and strontium ions removal from wastewater on gel and macroporous resins. Solv Extract Ion Exch 26:217–239
3. Zhang A, Wei Y, Hoshi H, Koma Y, Kamiya M (2007) Partitioning of cesium from a simulated high level liquid waste by extraction chromatography utilizing a macroporous silica-based supermolecular calix^{4}arene-crown impregnated polymeric composite. Solv Extract Ion Exch 25:389–405
4. El-Kamash AM, El-Naggar MR, El-Dessouky MI (2006) Immobilization of cesium and strontium radionuclides in zeolite-cement blends. J Hazard Mater 136:310–316

5. Gurboga G, Tel H, Altas Y (2006) Sorption studies of cesium on TiO$_2$–SiO$_2$ mixed gel spheres. Sep Purif Technol 47:96–104

6. Hassan NM, Adu-Wusu K, Nash CA, Marra JC (2004) Multiple ion exchange column tests for cesium removal from Hanford site tank 241-AW-101 with superLig® 644 resin. Solv Extract Ion Exch 22:979–996

7. Nilchi A, Malek B, Ghanadi M, Khanchi A (2003) Exchange properties of cyanide complex. Part I. Ion exchange of cesium on ferrocyanides. J Radioanal Nucl Chem 258:457–462

8. Mishra SP, Tiwari D (2002) Inorganic ion exchangers in radioactive waste management. J Radioanal Nucl Chem 253:421–426

9. Marinin DV, Brown GN (2000) Studies of sorbent/ion-exchange materials for the removal of radioactive strontium from liquid radioactive waste and high hardness ground waters. Waste Manag 20:545–553

10. Lehto J, Harjula R (1999) Selective separation of radionuclides from nuclear waste solutions with inorganic ion exchangers. Radiochim Acta 86:65–70

11. Rajec P, Matel L, Drechovska J, Sacha J, Navak I (1996) Sorption of radionuclides on inorganic sorbents. J Radioanal Nucl Chem Art 208:477–487

12. Motl M, John J, Šebesta F (1997) Composite absorbers of inorganic ion exchangers and polyacrylonitrile binding matrix. J Radioanal Nucl Chem 222:205–207

13. Narbbutt J, Bilewicz A, Baratos B (1989) Composite ion exchangers for radiocesium removal from nuclear reactor wastes. In: Proceedings of an international symposium on management of low and intermediate level radioactive wastes. IAEA, Vienna

14. Šebesta F, John J, Motl A, Watson J (1995) Development of PAN-based adsorbers for treating waste problems at U.S. DOE facilities. In: Proceedings of 5th international conference on radioactive waste management and environmental remediation, ICEM, pp 361–370

15. Nilchi A, Khanchi A, Atashi H, Bagheri A, Nematollahi L (2006) The application and properties of composite sorbents of inorganic ion exchangers and polyacrylonitrile binding matrix. J Hazard Mater 137:1271–1276

16. Ali IM, El-Zahhar AA, Zakaria ES (2005) Thermal and sorption behavior of polyacrylonitrile supported hydrous titanium dioxide. J Radioanal Nucl Chem 264:637–644

17. Kim HT, Lee CH, Shul YG, Moon JK, Lee EH (2003) Evaluation of PAN-TiO$_2$ composite adsorbent for removal of Pb(II) Ion in aqueous solution. Sep Purif Technol 38:695–713

18. Varshney KG, Tayal N, Khan AA, Niwas R (2001) Synthesis, characterization and analytical applications of lead (II) selective polyacrylonitrile thorium (IV) phosphate: a novel fibrous ion exchanger. Colloids Surf 181:123–129

19. Todd TA, Mann NR, Tranter TJ, Šebesta F, John J, Motl A (2002) Cesium sorption from concentrated acidic tank wastes using ammonium molybdophosphate-polyacrylonitrile composite sorbent. J Radioanal Nucl Chem 254:47–52

20. Someda HH, El-Zahhar AA, Shehata MK, El-Naggar HA (2002) Supporting of some ferrocyanides on polyacrylonitrile (PAN) binding polymer and their application for cesium treatment. Sep Purif Technol 29:53–61

21. Moon JK, Kim KW, Jung CH, Shul YG, Lee EH (2000) Preparation of organic-inorganic composite adsorbent beads for removal of radionuclides and heavy metal ions. J Radioanal Nucl Chem 246:299–307

22. Poojary DM, Cahill RA, Clearfield A (1996) Synthesis and structure of a layered titanosilicate catalyst with five-coordinate titanium. Natu Publ Grp 381:401–404

23. Celestian AJ, Medvedev DG, Tripathi A, Parise JB, Clearfield A (2005) Optimizing synthesis of Na$_2$Ti$_2$SiO$_7$·2H$_2$O (Na-CST) and ion exchange pathways for Cs$_{0.4}$H$_{1.6}$Ti$_2$SiO$_7$·H$_2$O (Cs-CST) determined from in situ synchrotron X-ray powder diffraction. Nucl Instrum Methods Phys Res B 238:61–69

24. Banerjee K, Amy GL, Prevost M, Nour S, Jekel M, Gallagher PM, Blumenschein CD (2008) Kinetic and thermodynamic aspects of adsorption of arsenic onto granular ferric hydroxide. Water Res 42:3371–3378

25. Langmuir I (1916) The constitution and fundamental properties of solids and liquids. J Am Chem Soc 38:2221–2295

26. Freundlich HMF (1906) Uber die adsorption in losungen. J Phys Chem 57:385–470